A circle-preserving C^2 Hermite interpolatory subdivision scheme with tension control

L. Romani [a,*]

[a] *Department of Mathematics and Applications, University of Milano-Bicocca, Via R. Cozzi 53, 20125 Milano, Italy*

Abstract

We present a tension-controlled 2-point Hermite interpolatory subdivision scheme that is capable of reproducing circles starting from a sequence of sample points with any arbitrary spacing and appropriately chosen first and second derivatives.

Whenever the tension parameter is set equal to 1, the limit curve coincides with the rational quintic Hermite interpolant to the given data and has guaranteed C^2 continuity, while for other positive tension values, continuity of curvature is conjectured and empirically shown by a wide range of experiments.

Key words: Rational interpolation, Hermite subdivision, curve fitting, circle-preserving, tension control.

1 Introduction

Subdivision algorithms are iterative methods for generating smooth curves and surfaces starting from a given polygonal control mesh.
Due to their efficiency, flexibility and simplicity, they have found their way into numerous applications in Computer Graphics and Computer-Aided Geometric Design.
While the popular spline-based schemes produce limit shapes that are much smaller than the starting mesh, interpolatory schemes suffer from the opposite problem: limit shapes tend to bulge out of the polygonal control mesh and they also frequently create undesirable oscillations. However, interpolatory schemes have attracted a lot of attention because they generate curves/surfaces passing through the vertices of the starting polygon/polyhedron. This is made possible by constructing rules

* Corresponding author.
Email address: lucia.romani@unimib.it (L. Romani).

that preserve the data points of the previous step. To additionally preserve other quantities, like first and second derivatives at these points, Hermite interpolatory subdivision schemes have been introduced (Merrien, 1992). They can be seen as a special case of vector subdivision schemes, where the components of each vector measure quantities with sensible geometric interpretation. Starting from an initial sequence of Hermite elements (i.e. vectors containing function values and associated derivatives), a Hermite subdivision scheme recursively generates finer sequences of Hermite elements which are associated with the midpoints of each span.
This paper is devoted to the design of a 2-point Hermite subdivision algorithm that, by simultaneously constructing points and associated derivatives, is able to produce tension-controlled C^2 interpolatory curves featured by the property of preservation of circles even when the given samples are not uniformly spaced. All these requests, considered of vital importance for curve design, can not be accomplished simultaneously by any of the existing scalar or vector interpolatory subdivision schemes. In fact, while the algorithms by Beccari et al. (2007), Chalmovianský & Jüttler (2007) and Sabin & Dodgson (2005) can generate exact circles, they are not C^2. Instead, although the proposals in Romani (2009) are tension-controlled C^2 improvements of the scheme in Beccari et al. (2007), they still suffer from the inability to reproduce circles from sequences of points that are not uniformly distributed.
On the other hand, none of the proposals of C^2 Hermite schemes appeared in the literature up to now (Merrien, 1999), is circle-preserving and tension-controlled at the same time.
Thus the subdivision scheme we are going to propose turns out to be unique in combining all the properties enumerated above. Moreover, for a certain value of the tension parameter, the constructed subdivision algorithm represents the first example of an interpolatory scheme converging towards a rational spline. In fact, while for approximating schemes there exist proposals generating rational curves (Farin and Nasri, 2001) or piecewise polynomials (think about the univariate versions of Doo-Sabin and Catmull-Clark subdivisions), it is not known any interpolatory subdivision algorithm capable of producing in the limit an intepolatory piecewise rational curve.
For all the issues considered, the discussed curve scheme thus compares favorably with the existing literature because it defines the first interpolatory model that is able to fulfill the list of all requirements identified as important for the use of subdivision methods in geometric modelling and engineering applications. In fact:

- it can exactly represent circles, which are considered fundamental shapes of great interest in CAGD;
- it can take advantage of a tension parameter that allows the user to control the shape of the limit curve;
- whenever the tension parameter is 1 it produces rational quintic splines and thus has guaranteed C^2-continuity (which is considered essential for serious design), while for arbitrary positive tension values it is empirically evident to be the case;
- it is able to solve the problem of artifact generation, frequently appearing in scalar interpolatory methods when dealing with a non-uniform distribution of

the starting points.

The paper is organized as follows. In Section 2, we describe a circle-preserving piecewise C^2 rational quintic Hermite interpolant. Then, in the two following sections, we derive the associated circle-preserving C^2 Hermite subdivision algorithm (Section 3), and we generalize its refinement rules to incorporate also non-spline cases (Section 4). The performed generalization is designed to enrich the scheme with the outstanding property of tension control. Finally, in Section 5, some examples are provided followed by further discussions and conclusions.

2 A circle-preserving piecewise C^2 rational Hermite interpolant

Let $\{\mathbf{f}_i^0\}_{i=0,\dots,N}$, $\{\mathbf{p}_i^0\}_{i=0,\dots,N}$ and $\{\mathbf{r}_i^0\}_{i=0,\dots,N}$, denote respectively an arbitrary sequence of interpolation points enumerated in counterclockwise order, and the associated first and second derivatives.
Our preliminary objective is to develop a C^2 solution to the interpolation problem of this data sequence, by means of a piecewise rational quintic made of pieces that join together with the so-called C^2 rational continuity (Hohmeyer and Barsky, 1989).
To construct our model, we need to define first a sequence of $N+1$ angular parameters σ which will be determined through the following procedure based on the `atan2` function. For the sake of generality, both the interpolation points and the associated derivatives will be defined in the 3D space via the notation $\mathbf{f}_i^0 := ((f_i^0)_x, (f_i^0)_y, (f_i^0)_z)$, $\mathbf{p}_i^0 := ((p_i^0)_x, (p_i^0)_y, (p_i^0)_z)$ and $\mathbf{r}_i^0 := ((r_i^0)_x, (r_i^0)_y, (r_i^0)_z)$, although the examples we will present in this paper are confined to the 2D case.

Algorithm 1 (*Angular parameters computation*)

(S.1) Compute the set of points $\{\mathbf{q}_i\}_{i=0,...,N}$ as the intersections of adjacent edge bisectors by exploiting the following formulas:

$\mathbf{f}^0_{-1} \equiv \mathbf{f}^0_N, \;\; \mathbf{f}^0_{N+1} \equiv \mathbf{f}^0_0$

`for` $i = 0, ..., N$

`if` $||(\mathbf{f}^0_{i-1} - \mathbf{f}^0_i) \times (\mathbf{f}^0_i - \mathbf{f}^0_{i+1})||^2_2 \neq 0$

$$\tau_1 = \frac{||\mathbf{f}^0_i - \mathbf{f}^0_{i+1}||^2_2 \, [(\mathbf{f}^0_{i-1} - \mathbf{f}^0_i) \cdot (\mathbf{f}^0_{i-1} - \mathbf{f}^0_{i+1})]}{2||(\mathbf{f}^0_{i-1} - \mathbf{f}^0_i) \times (\mathbf{f}^0_i - \mathbf{f}^0_{i+1})||^2_2}$$

$$\tau_2 = \frac{||\mathbf{f}^0_{i-1} - \mathbf{f}^0_{i+1}||^2_2 \, [(\mathbf{f}^0_i - \mathbf{f}^0_{i-1}) \cdot (\mathbf{f}^0_i - \mathbf{f}^0_{i+1})]}{2||(\mathbf{f}^0_{i-1} - \mathbf{f}^0_i) \times (\mathbf{f}^0_i - \mathbf{f}^0_{i+1})||^2_2}$$

$$\tau_3 = \frac{||\mathbf{f}^0_{i-1} - \mathbf{f}^0_i||^2_2 \, [(\mathbf{f}^0_{i+1} - \mathbf{f}^0_{i-1}) \cdot (\mathbf{f}^0_{i+1} - \mathbf{f}^0_i)]}{2||(\mathbf{f}^0_{i-1} - \mathbf{f}^0_i) \times (\mathbf{f}^0_i - \mathbf{f}^0_{i+1})||^2_2}$$

$$\mathbf{q}_i = \tau_1 \mathbf{f}^0_{i-1} + \tau_2 \mathbf{f}^0_i + \tau_3 \mathbf{f}^0_{i+1}$$

`else`

$$\mathbf{q}_i = \mathbf{f}^0_i$$

`end`

`end`

(S.2) Determine the barycenter $\mathbf{b} := ((b)_x, (b)_y, (b)_z)$ of the set of points $\{\mathbf{q}_i\}_{i=0,...,N}$.

(S.3) Let A be a $(N+1) \times 3$ matrix whose ith row is given by

$$[(f^0_i)_x - (b)_x, (f^0_i)_y - (b)_y, (f^0_i)_z - (b)_z], \quad i = 0, ..., N.$$

Calculate the "economy size" singular value decomposition (SVD) of A, namely in a Matlab-like notation

$$[U, S, V] = \text{svd}(A, 0)$$

where S is a 3×3 diagonal matrix with nonnegative diagonal elements in decreasing order and U and V are unitary matrices (U of the same dimension as A and V 3×3) so that $A = USV^T$.
In a Matlab-like notation, $\mathbf{n} := V(:, 3)$ is the right singular vector corresponding to the smallest singular value in S. Thus $\mathbf{n}$ identifies the direction cosines vector of the normal to the least-squares plane of the

points $\{\mathbf{f}_i^0\}_{i=0,\ldots,N}$, passing through $\mathbf{b}$. Hence $\mathbf{t}_0$ and $\mathbf{t}_1$ with

$$\mathbf{t}_0 = \frac{((n)_z,\, 0,\, -(n)_x)}{||\,((n)_z,\, 0,\, -(n)_x)\,||_2}, \quad \mathbf{t}_1 = \frac{(0,\, (n)_z,\, -(n)_y)}{||\,(0,\, (n)_z,\, -(n)_y)\,||_2}$$

are linear independent unit vectors that span such a plane.

(S.4) Let $\gamma_i := (\mathbf{f}_i^0 - \mathbf{b}) \cdot \mathbf{t}_0$ and $\mathbf{g}_i := (\mathbf{f}_i^0 - \mathbf{b}) \times \mathbf{t}_0$, $i = 0, ..., N$.
Then the sequence of angular parameters $\{\sigma_i\}_{i=0,\ldots,N}$ is worked out as follows:

$\mathbf{g}_{-1} \equiv \mathbf{g}_N, \quad \mathbf{g}_{N+1} \equiv \mathbf{g}_0$
`for` $i = 0, ..., N$
  `if` $\mathbf{g}_i \cdot \mathbf{n} \neq 0$
    $\sigma_i = -\text{atan2}(\mathbf{g}_i \cdot \mathbf{n}, \gamma_i)$
  `else`
    `if` $\mathbf{g}_{i-1} \cdot \mathbf{n} < 0$ `&` $\mathbf{g}_{i+1} \cdot \mathbf{n} > 0$
      $\sigma_i = \pi$ [with the exception $\sigma_i = -\pi$ when $i = 0$]
    `else`
      $\sigma_i = 0$
    `end`
  `end`
`end`

Remark 1 *Although step* **(S.1)** *solves the divide-by-zero problem arising in case of collinear vertices* $\mathbf{f}_i^0 s$*, dealing with starting polylines with nearly collinear points could lead to numerical instability in the computation of the* $\mathbf{q}_i s$*. Thus it is our future intention to address this problem in order to extend the applicability of Algorithm 1.*
Additionally, another possible direction for future improvement of this procedure concerns the fulfilment of the property of rotation invariance, which is currently lost when one of the vertices $\mathbf{f}_i^0$ *coincides with the barycenter, due to the assignment* $\sigma_i = 0$ *or* $\pm\pi$ *in step* **(S.4)**.

Algorithm 1 provides a vector σ of angles expressed in radians, which, according to the output of the `atan2` function, are confined to the range $[-\pi, \pi]$. Since they correspond to the angles $\angle(\mathbf{f}_i^0 - \mathbf{b}, \mathbf{t}_0)$, $i = 0, ..., N$, depending on the distribution of the assigned points $\{\mathbf{f}_i^0\}_{i=0,\ldots,N}$, the σ_i values may be in ascending order or not. Clearly, if this is not the case, the σ_i values should be opportunely shifted in order to satisfy the constraint $\sigma_i < \sigma_{i+1}$ for all i.
Once the assigned points $\{\mathbf{f}_i^0\}_{i=0,\ldots,N}$ are associated with σ_i values in ascending order, we can extend the results in Casciola and Romani (2005), to define a piecewise rational quintic Hermite interpolant to the given data. Assuming the notation

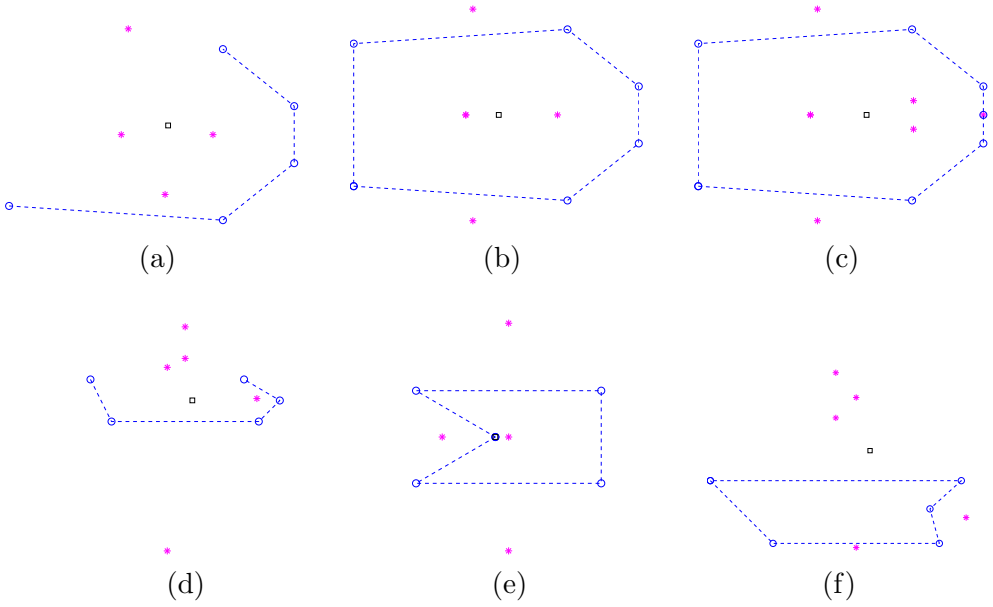

Fig. 1. Examples of 2D interpolating points $\mathbf{f}_i^0$ (small circles) with the associated $\mathbf{q}_i$ (asterisks) and their barycenter $\mathbf{b}$ (open square). Note how some of the $\mathbf{q}_i$s may be coincident and the barycenter position may move from inside to outside, also passing through one of the polyline vertices, depending on their distribution.

$$\alpha_i = \tan\left(\frac{\sigma_i}{4}\right), \tag{1}$$

the key idea is thus to identify by the interval $\left[\frac{1+\alpha_i}{2}, \frac{1+\alpha_{i+1}}{2}\right] \subset [0,1]$ the domain of each rational curve segment $\mathbf{c}_i(t) : \left[\frac{1+\alpha_i}{2}, \frac{1+\alpha_{i+1}}{2}\right] \to \mathbb{R}^3$, that has to satisfy the following interpolation conditions at the endpoints:

$$\mathbf{c}_i\left(\frac{1+\alpha_{i+j}}{2}\right) = \mathbf{f}_{i+j}^0, \quad \mathbf{c}_i'\left(\frac{1+\alpha_{i+j}}{2}\right) = \mathbf{p}_{i+j}^0, \quad \mathbf{c}_i''\left(\frac{1+\alpha_{i+j}}{2}\right) = \mathbf{r}_{i+j}^0, \quad j = 0, 1. \tag{2}$$

Remark 2 *Note that, for the sake of conciseness, the three interpolation conditions to be satisfied at each endpoint have been expressed in a unified form by letting the index j assume the value 0 or 1. Also in the sequel, whenever the notation $j = 0, 1$ is used, we intend to incorporate conditions for the two endpoints in a single equation.*

Since the definition of a rational Bézier representation with finite control points relies on positive weights, the following Lemma is devoted to show positivity of the sextuple we will assume as weight vector for each single Bézier piece.

Lemma 3 *Let σ_i $(i = 0, ..., N)$ be the angular parameters determined through Algorithm 1 and denote by α_i the tangent values computed by formula (1). Then each*

sextuple

$$\begin{aligned}
\mu_0^i &= \tfrac{1}{4}(\alpha_i^2+1)^2,\\
\mu_1^i &= \tfrac{1}{20}(\alpha_i^2+1)(\alpha_i^2+4\alpha_{i+1}\alpha_i+5),\\
\mu_2^i &= \tfrac{1}{20}[\alpha_{i+1}^2(3\alpha_i^2+1)+2\alpha_i\alpha_{i+1}(\alpha_i^2+3)+(3\alpha_i^2+5)],\\
\mu_3^i &= \tfrac{1}{20}[\alpha_i^2(3\alpha_{i+1}^2+1)+2\alpha_{i+1}\alpha_i(\alpha_{i+1}^2+3)+(3\alpha_{i+1}^2+5)],\\
\mu_4^i &= \tfrac{1}{20}(\alpha_{i+1}^2+1)(\alpha_{i+1}^2+4\alpha_i\alpha_{i+1}+5),\\
\mu_5^i &= \tfrac{1}{4}(\alpha_{i+1}^2+1)^2
\end{aligned} \tag{3}$$

is defined by only positive scalars.

PROOF. As computed in step (**S.4**), the angular parameters $\sigma_i \in [-\pi,\pi]$, hence the tangent values α_i defined through (1) are in $[-1,1]$. Therefore, looking at $\mu_0^i,...,\mu_5^i$ as functions of the two variables $\alpha_i,\ \alpha_{i+1}$ defined in the domain $[-1,1]^2$, it turns out that they are all strictly positive and in particular assume the minimum values $\frac{1}{4},\ \frac{1}{5},\ \frac{1}{5},\ \frac{1}{5},\ \frac{1}{5},\ \frac{1}{4}$ respectively. Hence the thesis trivially follows. □

At this point, all the requirements in (2) can be fulfilled by expressing $\mathbf{c}_i(t)$ as in the forthcoming definition.

Definition 4 *Let $\mathbf{f}_i^0$, $\mathbf{p}_i^0$, and $\mathbf{r}_i^0$ $(i=0,...,N)$ be the sequence of interpolating data and the associated first and second order derivatives. Having computed the angular parameters σ_i $(i=0,...,N)$ through Algorithm 1 and denoted by α_i the correspondent tangent values in (1), we define by $\mathbf{c}(t)$ the piecewise rational quintic Bézier curve whose segments $\mathbf{c}_i(t):\left[\frac{1+\alpha_i}{2},\frac{1+\alpha_{i+1}}{2}\right]\to\mathbb{R}^3$ $(i=0,...,N-1)$ have the form*

$$\mathbf{c}_i(t)=\sum_{k=0}^{5}\mathbf{Q}_k^i\ R_{k,5}^i(t) \tag{4}$$

where

$$\begin{aligned}
\mathbf{Q}_0^i &= \mathbf{f}_i^0,\\
\mathbf{Q}_1^i &= \mathbf{f}_i^0+\tfrac{(\alpha_{i+1}-\alpha_i)\ \mu_0^i}{10\mu_1^i}\ \mathbf{p}_i^0,\\
\mathbf{Q}_2^i &= \mathbf{f}_i^0+\tfrac{\left(5\mu_1^i-\mu_0^i\right)(\alpha_{i+1}-\alpha_i)}{20\mu_2^i}\ \mathbf{p}_i^0+\tfrac{(\alpha_{i+1}-\alpha_i)^2\ \mu_0^i}{80\mu_2^i}\ \mathbf{r}_i^0,\\
\mathbf{Q}_3^i &= \mathbf{f}_{i+1}^0-\tfrac{\left(5\mu_4^i-\mu_5^i\right)(\alpha_{i+1}-\alpha_i)}{20\mu_3^i}\ \mathbf{p}_{i+1}^0+\tfrac{(\alpha_{i+1}-\alpha_i)^2\ \mu_5^i}{80\mu_3^i}\ \mathbf{r}_{i+1}^0,\\
\mathbf{Q}_4^i &= \mathbf{f}_{i+1}^0-\tfrac{(\alpha_{i+1}-\alpha_i)\ \mu_5^i}{10\mu_4^i}\ \mathbf{p}_{i+1}^0,\\
\mathbf{Q}_5^i &= \mathbf{f}_{i+1}^0,
\end{aligned} \tag{5}$$

$\{\mu_k^i\}_{k=0,...,5}$ are the positive weights introduced in (3) and $\{R_{k,5}^i(t)\}_{k=0,...,5}$ the ra-

tional quintic Bézier polynomials defined by the expression

$$R^i_{k,5}(t) = \frac{\mu^i_k B^i_{k,5}(t)}{\sum_{\ell=0}^{5} \mu^i_\ell B^i_{\ell,5}(t)}, \tag{6}$$

with

$$B^i_{k,5}(t) = \binom{5}{k} \frac{(1+\alpha_{i+1}-2t)^{5-k}\ (2t-\alpha_i-1)^k}{(\alpha_{i+1}-\alpha_i)^5}. \tag{7}$$

We will now show that the rational quintic Hermite segment introduced in Definition 4 can be used for precisely representing any arbitrary circle arc.

Proposition 5 *Let ρ be a positive real number. The rational quintic Hermite segment $\mathbf{c}_i(t) : \left[\frac{1+\alpha_i}{2}, \frac{1+\alpha_{i+1}}{2}\right] \to \mathbb{R}^2$ interpolating the data*

$$\begin{aligned}
(f^0_{i+j})_x &= \rho \tfrac{[(\alpha_{i+j})^2+2\alpha_{i+j}-1][(\alpha_{i+j})^2-2\alpha_{i+j}-1]}{[(\alpha_{i+j})^2+1]^2} \\
(f^0_{i+j})_y &= -4\rho \tfrac{\alpha_{i+j}(\alpha_{i+j}+1)(\alpha_{i+j}-1)}{[(\alpha_{i+j})^2+1]^2}
\end{aligned}$$

$$\begin{aligned}
(p^0_{i+j})_x &= 32\rho \tfrac{\alpha_{i+j}(\alpha_{i+j}+1)(\alpha_{i+j}-1)}{[(\alpha_{i+j})^2+1]^3} \qquad \text{for } j = 0, 1 \\
(p^0_{i+j})_y &= 8\rho \tfrac{[(\alpha_{i+j})^2+2\alpha_{i+j}-1][(\alpha_{i+j})^2-2\alpha_{i+j}-1]}{[(\alpha_{i+j})^2+1]^3}
\end{aligned}$$

$$\begin{aligned}
(r^0_{i+j})_x &= -64\rho \tfrac{[3(\alpha_{i+j})^4-8(\alpha_{i+j})^2+1]}{[(\alpha_{i+j})^2+1]^4} \\
(r^0_{i+j})_y &= -32\rho \tfrac{\alpha_{i+j}[(\alpha_{i+j})^4-14(\alpha_{i+j})^2+9]}{[(\alpha_{i+j})^2+1]^4}
\end{aligned}$$

allows us to exactly represent any arbitrary circle arc of radius ρ and center $(0,0)$.

PROOF. Writing the rational quintic Hermite interpolatory model of Definition 4 by using the data above, we obtain an expression of $\mathbf{c}_i(t)$ whose x and y components turn out to satisfy the canonical equation $[(c_i(t))_x]^2 + [(c_i(t))_y]^2 = \rho^2$ corresponding to a circular arc of radius ρ and center $(0,0)$. □

However, like in the very general case, also the capability of representing a specific circle arc is subject to the constraint of possessing endpoints with angular parameters satisfying the condition $\sigma_i, \sigma_{i+1} \in [-\pi, \pi]$ and $\sigma_i < \sigma_{i+1}$.
Thus, in the forthcoming section, we will provide a more robust solution to this Hermite-type interpolation problem that is capable of achieving circular precision whenever the input data come from a circular arc. It will consist in a Hermite subdivision algorithm that, starting from an arbitrary sequence of points and associated derivatives ordered counterclockwise, generates a smooth limit curve interpolating

the given data.
A necessary step for extending the applicability of the new algorithm to any set of vertices, is the enlargement of the angular parameters range computed through Algorithm 1 to the interval $]-2\pi, 2\pi[$, in such a way that the σ_i values can be sorted in ascending order without losing the ordering of the assigned data. This is done in step **(S.5)**, as described in the sequel.

(S.5) Extension of the angular parameters computed in step **(S.4)** to the range $]-2\pi, 2\pi[$:

```
for   i = 0, ..., N − 1
      if  σ_i > σ_{i+1}
          ī = i + 1
          break
      else
          ī = N + 1
      end
end
for   i = ī, ..., N
      σ_i = σ_i + 2π
end
```

Note that, in case $\sigma_N \geq 2\pi$, we have to shift back the σ vector by 2π, namely we set $\sigma = \sigma - 2\pi$.

We further observe that, if the starting polyline is self-intersecting (see Fig. 2), there could be more than one index $\bar{i}$ where $\sigma_i > \sigma_{i+1}$ occurs. In this case, it is sufficient to add to the σ_is successive multiples of 2π in order to get an increasing sequence of values. Then we map the σ vector into the interval $[-\pi, \pi]$ by computing $\frac{(\sigma_i - \sigma_0)2\pi}{\sigma_N - \sigma_0} - \pi$ for all $i = 0, ..., N$.

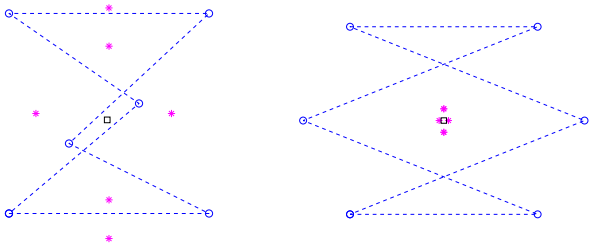

Fig. 2. Examples of self-intersecting polylines with the associated $\mathbf{q}_i$s (asterisks) and their barycenter $\mathbf{b}$ (open square).

3 A circle-preserving 2-point Hermite-interpolatory subdivision algorithm

The important schemes for applications are required to be sufficiently smooth (C^2 is highly desirable) and capable of reproducing curves widely used in Computer-Aided Design, such as circles. Thus in this section we will derive the refinement rules of a circle-preserving C^2 Hermite-interpolatory subdivision algorithm that is able to reproduce circles starting from points lying on it with any arbitrary spacing. This novel set of refinement equations will be derived by dyadically sampling from the piecewise rational quintic Bézier curve described in Section 2.

As it happens with any standard Hermite subdivision scheme, we start knowing the values of a function f and of its first and second derivatives $p = f'$, $r = f''$ at the endpoints of a bounded interval $I = [a, b]$ of $\mathbb{R}$. Then, given $(f(a), p(a), r(a))$ and $(f(b), p(b), r(b))$, to build f, p and r on I, we proceed recursively by induction on $k \in \mathbb{N} \cup \{0\}$. More precisely, at step k we denote by $\mathcal{D}_k = \{\nu_i^k = a + i(b-a)/2^k\}_{i=0,1,\dots,2^k}$ the regular partition of I in 2^k subintervals and we assume that f, p, r are already known on its points. If c and d are two consecutive points of $\mathcal{D}_k$, then we compute f, p and r at the midpoint $(c+d)/2 \in \mathcal{D}_{k+1} \backslash \mathcal{D}_k$ according to the following scheme, which depends on a parameter matrix $\Lambda^{k+1} = (\lambda_{h\ell}^{k+1})_{h=0,\dots,2,\ \ell=0,\dots,5}$:

$$
\begin{aligned}
f\left(\tfrac{c+d}{2}\right) &= \lambda_{00}^{k+1} f(c) + \lambda_{01}^{k+1} f(d) + \lambda_{02}^{k+1} p(c) + \lambda_{03}^{k+1} p(d) + \lambda_{04}^{k+1} r(c) + \lambda_{05}^{k+1} r(d) \\
p\left(\tfrac{c+d}{2}\right) &= \lambda_{10}^{k+1} f(c) + \lambda_{11}^{k+1} f(d) + \lambda_{12}^{k+1} p(c) + \lambda_{13}^{k+1} p(d) + \lambda_{14}^{k+1} r(c) + \lambda_{15}^{k+1} r(d) \\
r\left(\tfrac{c+d}{2}\right) &= \lambda_{20}^{k+1} f(c) + \lambda_{21}^{k+1} f(d) + \lambda_{22}^{k+1} p(c) + \lambda_{23}^{k+1} p(d) + \lambda_{24}^{k+1} r(c) + \lambda_{25}^{k+1} r(d).
\end{aligned}
\tag{8}
$$

By applying these formulae on ever finer partitions, we define f, p and r on $\mathcal{D} = \bigcup_k \mathcal{D}_k$ which is a dense subset of I. We say that the scheme (8) is C^2 convergent if, for any initial data, f, p and r can be extended from $\mathcal{D}$ to continuous functions on I with $p = f'$ and $r = f''$.

f, defined either on I or on $\mathcal{D}$, is called the HC^2 interpolant to the data.

The HC^2 algorithm in (8) can also be formulated as follows. We start with Hermite data f_0, p_0, r_0, f_1, p_1, r_1 at the endpoints of a finite interval $[a, b]$ and set $f_0^0 = f_0$, $p_0^0 = p_0$, $r_0^0 = r_0$, $f_1^0 = f_1$, $p_1^0 = p_1$, $r_1^0 = r_1$. For $k \geq 0$ and $i = 0, 1, ..., 2^k - 1$

$$
\begin{aligned}
f_{2i}^{k+1} &= f_i^k \\
p_{2i}^{k+1} &= p_i^k \\
r_{2i}^{k+1} &= r_i^k \\
f_{2i+1}^{k+1} &= \lambda_{00}^{k+1} f_i^k + \lambda_{01}^{k+1} f_{i+1}^k + \lambda_{02}^{k+1} p_i^k + \lambda_{03}^{k+1} p_{i+1}^k + \lambda_{04}^{k+1} r_i^k + \lambda_{05}^{k+1} r_{i+1}^k \\
p_{2i+1}^{k+1} &= \lambda_{10}^{k+1} f_i^k + \lambda_{11}^{k+1} f_{i+1}^k + \lambda_{12}^{k+1} p_i^k + \lambda_{13}^{k+1} p_{i+1}^k + \lambda_{14}^{k+1} r_i^k + \lambda_{15}^{k+1} r_{i+1}^k \\
r_{2i+1}^{k+1} &= \lambda_{20}^{k+1} f_i^k + \lambda_{21}^{k+1} f_{i+1}^k + \lambda_{22}^{k+1} p_i^k + \lambda_{23}^{k+1} p_{i+1}^k + \lambda_{24}^{k+1} r_i^k + \lambda_{25}^{k+1} r_{i+1}^k
\end{aligned}
\tag{9}
$$

and $f_{2^{k+1}}^{k+1} = f_{2^k}^k$, $p_{2^{k+1}}^{k+1} = p_{2^k}^k$, $r_{2^{k+1}}^{k+1} = r_{2^k}^k$.

If the scheme is C^2 convergent with limit functions f, p and r, then

$$
f(\nu_i^k) = f_i^k, \quad f'(\nu_i^k) = p_i^k, \quad f''(\nu_i^k) = r_i^k, \quad \nu_i^k = a + i\,\frac{b-a}{2^k}, \quad i = 0, 1, ..., 2^k.
$$

As concerns all the 2-point Hermite subdivision schemes appeared in the literature up to now, the parameter matrix Λ^{k+1} is defined by coefficients which satisfy the following relations

$$
\begin{aligned}
&\lambda_{01}^{k+1} = \lambda_{00}^{k+1} = \tfrac{1}{2}, \quad && \lambda_{03}^{k+1} = -\lambda_{02}^{k+1}, \quad && \lambda_{05}^{k+1} = \lambda_{04}^{k+1} \\
&\lambda_{11}^{k+1} = -\lambda_{10}^{k+1}, && \lambda_{13}^{k+1} = \lambda_{12}^{k+1}, && \lambda_{15}^{k+1} = -\lambda_{14}^{k+1} \\
&\lambda_{21}^{k+1} = \lambda_{20}^{k+1} = 0, && \lambda_{23}^{k+1} = -\lambda_{22}^{k+1}, && \lambda_{25}^{k+1} = \lambda_{24}^{k+1}.
\end{aligned}
\tag{10}
$$

We will now show that it is possible to construct a Hermite subdivision scheme HS22 whose coefficients matrix does not follow the pattern in (10).
This occurs by deriving a 2-point Hermite subdivision scheme featured by the property of circle-preservation and by the peculiarity of converging to the rational quintic Hermite interpolant in Definition 4, where it exists. In fact, if for such a rational Bézier curve, we perform the insertion of a 5-fold knot at the midpoint of the underlying knot-interval, after some algebraic manipulations we arrive at formulating the new point and derivatives at the midknot in terms of the Hermite data associated with the endpoints of the knot-interval, as expressed in formula (9). In particular, after having introduced the following notation

$$
\begin{aligned}
\phi_1(u,v) &= \frac{[(3-5v^2+8v^4)u^6-16v(1-2v^2)u^5-(2-43v^2+3v^4)u^4+16v(1-v^2)u^3+}{16(uv+1)^5(uv-1)} \\
&\quad \frac{+(3-43v^2+2v^4)u^2-16v(2-v^2)u-8+5v^2-3v^4](v^2+1)}{16(uv+1)^5(uv-1)} \\
\phi_2(u,v) &= \frac{(u^2+1)(u-v)[(5v^2-3)u^2+16uv-3v^2+5](v^2+1)^2}{32(uv+1)^4(v-1)(v+1)(uv-1)} \\
\phi_3(u,v) &= \frac{(v^2+1)^4(v-u)^2(u^2+1)}{64(uv+1)^3(v-1)^3(v+1)^3(uv-1)} \\
\phi_4(u,v) &= \frac{[(-5v^2+3)(3v^4+1)u^6-16v(3v^4-2v^2+1)u^5+(9v^6-39v^4+43v^2-5)u^4+}{8(uv+1)^5(v-u)} \\
&\quad \frac{+32v(v^4+1)u^3-(5v^6-43v^4+39v^2-9)u^2-16v(v^4-2v^2+3)u+(3v^2-5)(v^4+3)]}{8(uv+1)^5(v-u)} \\
\phi_5(u,v) &= \frac{[(-7u^4+6u^2-3)v^2-16u(u^2-1)v-6u^2+3u^4+7](v^2+1)^2}{16(uv+1)^4(v-1)(v+1)} \\
\phi_6(u,v) &= \frac{(u-1)(u+1)(v^2+1)^4(v-u)}{32(uv+1)^3(v-1)^3(v+1)^3} \\
\phi_7(u,v) &= \frac{3(uv-1)^3(u+v)(uv-v+u+1)(uv+v-u+1)}{(uv+1)^5(u-v)} \\
\phi_8(u,v) &= \frac{3(uv-1)^3(uv-v+u+1)(uv+v-u+1)(v^2+1)}{2(uv+1)^4(v-u)(v-1)(v+1)} \\
\phi_9(u,v) &= \frac{(1-uv)^3(v^2+1)^3}{4(uv+1)^3(v-1)^3(v+1)^3},
\end{aligned}
\tag{11}
$$

for all $k \geq 0$ the coefficients $\{\lambda_{h\ell}^{k+1}\}_{h=0,\ldots,2,\ \ell=0,\ldots,5}$ in (9) are defined by

$$
\begin{aligned}
&\lambda_{00}^{k+1} = 1-\phi_1(s_{i+1}^{k+1}, s_i^{k+1}),\ \lambda_{01}^{k+1} = \phi_1(s_{i+1}^{k+1}, s_i^{k+1}), \\
&\lambda_{02}^{k+1} = \phi_2(s_{i+1}^{k+1}, s_i^{k+1}), \qquad \lambda_{03}^{k+1} = \phi_2(s_i^{k+1}, s_{i+1}^{k+1}), \\
&\lambda_{04}^{k+1} = \phi_3(s_{i+1}^{k+1}, s_i^{k+1}), \qquad \lambda_{05}^{k+1} = \phi_3(s_i^{k+1}, s_{i+1}^{k+1}), \\
&\lambda_{10}^{k+1} = -\phi_4(s_{i+1}^{k+1}, s_i^{k+1}), \quad \lambda_{11}^{k+1} = \phi_4(s_{i+1}^{k+1}, s_i^{k+1}), \\
&\lambda_{12}^{k+1} = \phi_5(s_{i+1}^{k+1}, s_i^{k+1}), \qquad \lambda_{13}^{k+1} = \phi_5(s_i^{k+1}, s_{i+1}^{k+1}), \\
&\lambda_{14}^{k+1} = \phi_6(s_{i+1}^{k+1}, s_i^{k+1}), \qquad \lambda_{15}^{k+1} = \phi_6(s_i^{k+1}, s_{i+1}^{k+1}), \\
&\lambda_{20}^{k+1} = -\phi_7(s_{i+1}^{k+1}, s_i^{k+1}), \quad \lambda_{21}^{k+1} = \phi_7(s_{i+1}^{k+1}, s_i^{k+1}), \\
&\lambda_{22}^{k+1} = \phi_8(s_{i+1}^{k+1}, s_i^{k+1}), \qquad \lambda_{23}^{k+1} = \phi_8(s_i^{k+1}, s_{i+1}^{k+1}), \\
&\lambda_{24}^{k+1} = \phi_9(s_{i+1}^{k+1}, s_i^{k+1}), \qquad \lambda_{25}^{k+1} = \phi_9(s_i^{k+1}, s_{i+1}^{k+1})
\end{aligned}
\tag{12}
$$

where

$$
s_i^{k+1} = \tan(\sigma_i^{k+1}) \tag{13}
$$

and

$$\begin{aligned} &\sigma_i^1 = \tfrac{\sigma_i}{8} \\ &\sigma_{2i}^{k+1} = \sigma_i^k, \quad \sigma_{2i+1}^{k+1} = \tfrac{\sigma_i^k + \sigma_{i+1}^k}{2} \quad \text{when } k \geq 1. \end{aligned} \tag{14}$$

Remark 6 *Whenever* $\sigma_{i+1}^{k+1} = -\sigma_i^{k+1}$ *(namely* $s_{i+1}^{k+1} = -s_i^{k+1}$*) the coefficients matrix* Λ^{k+1} *has the structure in (10).*

3.1 Reproduction of circles

Let $\{\mathbf{f}_i^0\}_{i=0,\ldots,N}$ $(N \geq 2)$ be a given sequence of starting points. If they lie on a circle, the point $\mathbf{b} = ((b)_x, (b)_y)$ computed in step **(S.2)** of Algorithm 1 coincides with its center, and its radius is given by

$$\rho = \sqrt{[(f_0^0)_x - (b)_x]^2 + [(f_0^0)_y - (b)_y]^2}.$$

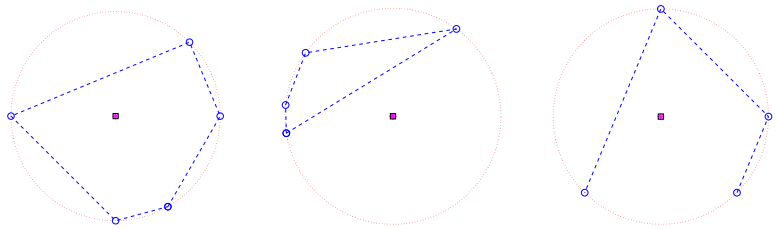

Fig. 3. Examples of sequences of interpolating points $\mathbf{f}_i^0$ lying on a circle, with the associated set of coincident points $\mathbf{q}_i$ (asterisks) and their barycenter $\mathbf{b}$ (open square).

Once $\mathbf{b}$ and ρ have been determined, we can then work out the $\{\sigma_i\}_{i=0,\ldots,N}$ vector through Algorithm 1. Being σ_i and σ_{i+1} the angular parameters for the endpoints $\mathbf{f}_i^0$ and $\mathbf{f}_{i+1}^0$, they turn out to fulfill the following equations

$$\begin{aligned} (f_{i+j}^0)_x &= \rho \tfrac{(s_{i+j}^1)^8 - 28(s_{i+j}^1)^6 + 70(s_{i+j}^1)^4 - 28(s_{i+j}^1)^2 + 1}{[(s_{i+j}^1)^2 + 1]^4} \\ &\qquad\qquad \text{for } j = 0, 1 \\ (f_{i+j}^0)_y &= -8\rho \tfrac{s_{i+j}^1[(s_{i+j}^1)^6 - 7(s_{i+j}^1)^4 + 7(s_{i+j}^1)^2 - 1]}{[(s_{i+j}^1)^2 + 1]^4} \end{aligned}$$

with s_i^1 given by (13) for $k = 0$ and $\sigma_i^1 = \frac{\sigma_i}{8}$.
Hence, in order to reproduce the circular segment confined between the two points, it is necessary to define the associated first and second derivatives through the formulae

$$(p^0_{i+j})_x = 64\rho \frac{s^1_{i+j}[(s^1_{i+j})^2-1]^3[(s^1_{i+j})^2+2(s^1_{i+j})-1][(s^1_{i+j})^2-2(s^1_{i+j})-1]}{[(s^1_{i+j})^2+1]^6}$$

$$(p^0_{i+j})_y = 8\rho \frac{[(s^1_{i+j})^2-1]^2[(s^1_{i+j})^4-4(s^1_{i+j})^3-6(s^1_{i+j})^2+4(s^1_{i+j})+1][(s^1_{i+j})^4+4(s^1_{i+j})^3-6(s^1_{i+j})^2-4(s^1_{i+j})+1]}{[(s^1_{i+j})^2+1]^6}$$

for $j = 0, 1$.

$$(r^0_{i+j})_x = -64\rho \frac{[(s^1_{i+j})^2-1]^4[(s^1_{i+j})^8-36(s^1_{i+j})^6+118(s^1_{i+j})^4-36(s^1_{i+j})^2+1]}{[(s^1_{i+j})^2+1]^8}$$

$$(r^0_{i+j})_y = 64\rho \frac{s^1_{i+j}[(s^1_{i+j})^2-1]^3[9(s^1_{i+j})^8-92(s^1_{i+j})^6+182(s^1_{i+j})^4-92(s^1_{i+j})^2+9]}{[(s^1_{i+j})^2+1]^8}$$

Then, starting from these Hermite data, the refinement algorithm in (9) is able to generate the exact circle arc confined between $(\mathbf{f}^0_i, \mathbf{p}^0_i, \mathbf{r}^0_i)$ and $(\mathbf{f}^0_{i+1}, \mathbf{p}^0_{i+1}, \mathbf{r}^0_{i+1})$. A simple proof of this result is given by the identity $\left[\left(f^{k+1}_{2i+1}\right)_x\right]^2 + \left[\left(f^{k+1}_{2i+1}\right)_y\right]^2 = \rho^2$ for all $k \geq 0$.

4 A tension-controlled generalization of the spline-based Hermite subdivision algorithm

Let $w > 0$ be a free parameter to be chosen by the user. If, for all $k \geq 0$, we replace s^{k+1}_{i+1} by $ws^{k+1}_{i+1} + (1-w)s^{k+1}_i$ in all the equations (12) identifying the coefficients $\{\lambda^{k+1}_{h\ell}\}_{h=0,\ldots,2,\ \ell=0,\ldots,5}$, then the refinement rules (9) will contain the free parameter w. Note that, whenever $w = 1$, the generalized Hermite scheme goes back to the spline-based one introduced in the previous section, and therefore it converges to the piecewise rational Hermite interpolant of Section 2; thus, if the starting points lie on a circle, the subdivision algorithm will be able to reproduce it (Figs. 4-5). Moreover, the obtained generalization further possesses the property of tension control. In fact, while choosing w closer and closer to 0, we get a limit curve that increasingly approaches to the starting control polyline, for larger and larger values of w we generate looser and looser shapes (Fig. 9).

An open question, that naturally arises, is if the limit curve produced by the generalized scheme is C^2 for any positive value of the parameter w. By construction, we can assert that the smoothness order of the limit curve is 2 whenever $w = 1$, since in this case we know that this is exactly the C^2 piecewise rational quintic Bézier curve. For any other positive value of w, a detailed smoothness analysis should be performed. But, because the refinement equations of this Hermite scheme are not in the same form of the ones presented and analyzed in the literature up to now (Dyn and Levin, 1999; Dubuc et al., 2001; Yu, 2005; Dubuc, 2006), at this moment there are not the required tools to give a precise answer. However, all our experimental results let us conjecture that curvature continuity is preserved for any choice of

$w > 0$. In fact, the discrete curvature plots obtained after a certain number of steps of the proposed subdivision algorithm for different starting polylines and arbitrarily chosen tension values, turn out to be always continuous (see Section 5).

5 Numerical examples

This section is devoted to the illustration of some numerical examples confirming the effectiveness of the proposed 2-point Hermite-interpolatory subdivision scheme (Figs. 4, 5, 6, 7, 8, 9).

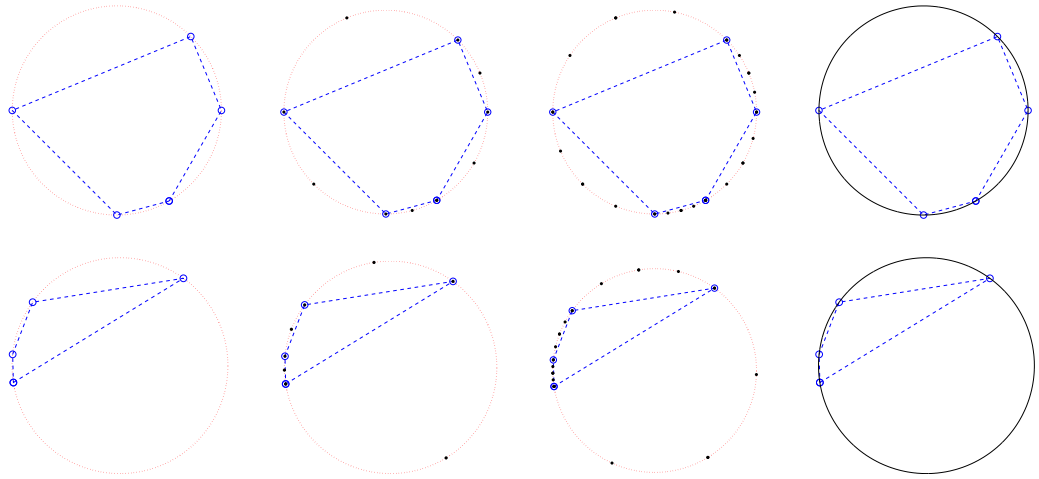

Fig. 4. Exact reconstruction of the full circle from non-regular closed polylines. From left to right: starting polyline, points at 1st and 2nd level of refinement, refined polyline after 10 steps of the algorithm.

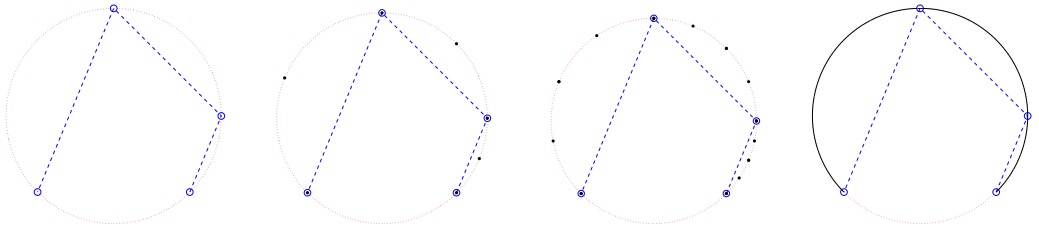

Fig. 5. Exact reconstruction of a circular arc from a non-regular open polyline. From left to right: starting polyline, points at 1st and 2nd level of refinement, refined polyline after 10 steps of the algorithm.

Due to the fact that the novel refinement rules are built upon a piecewise C^2 Hermite interpolant, they should naturally guarantee a C^2 limit curve for any positive value of w. For the particular starting polylines in Fig. 9, curvature continuity is demonstrated by the curvature plots in Fig. 10.

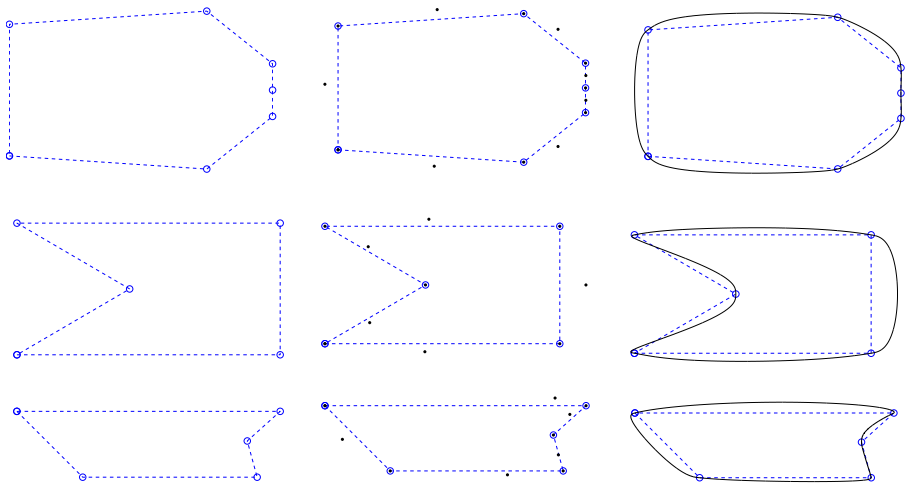

Fig. 6. Subdivision of non-regular closed polylines. From left to right: starting polyline, points at 1st level of refinement, refined polyline after 10 steps of the algorithm.

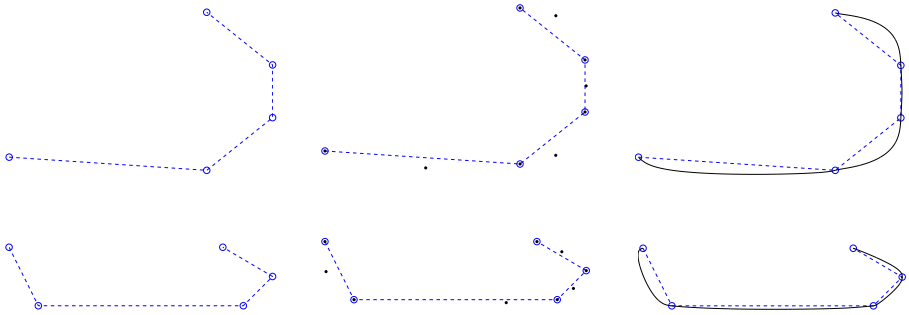

Fig. 7. Subdivision of non-regular open polylines. From left to right: starting polyline, points at 1st level of refinement, refined polyline after 10 steps of the algorithm.

6 Conclusions and further research

Stimulated by the observation that C^2 smoothness is considered essential for serious design and piecewise polynomial reproduction is one of the very important requirements in geometric modelling applications, we have proposed a 2-point C^2 Hermite interpolatory subdivision scheme whose refinement rules go back to a piecewise C^2 rational quintic Bézier interpolant. But although these two aspects clearly have a decisive impact on the quality of the limit curve, they are by no means the only important factors. In fact, the preservation of relevant shapes in CAGD (like circles) and the possibility of controlling the behaviour of the limit curve in an intuitive way, are also considered equally significant. Thus, the refinement equations of the proposed scheme have been conceived in such a way that exact circles can be naturally reproduced starting by any arbitrarily-spaced sequence of points sampled on it, and successively generalized to contain a free parameter w that allows the user to manipulate tension effects. In particular, while for smaller and smaller values of

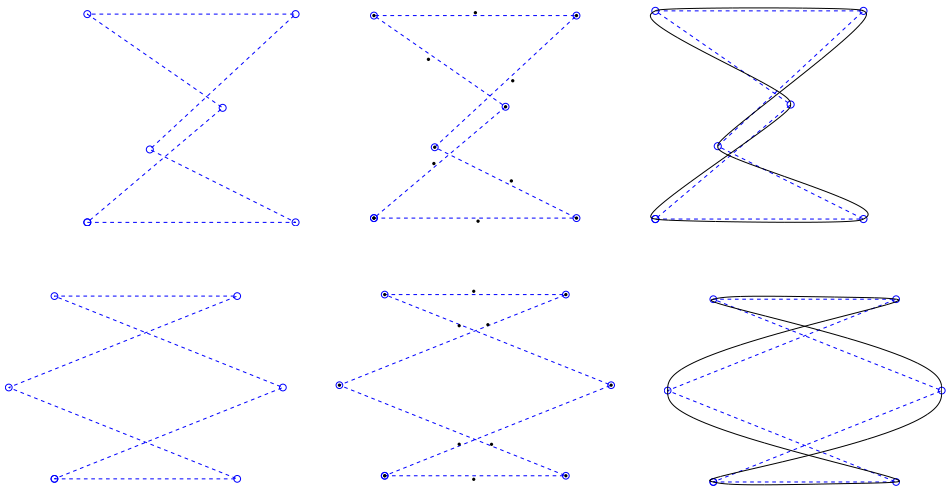

Fig. 8. Subdivision of non-regular self-intersecting polylines. From left to right: starting polyline, points at 1st level of refinement, refined polyline after 10 steps of the algorithm.

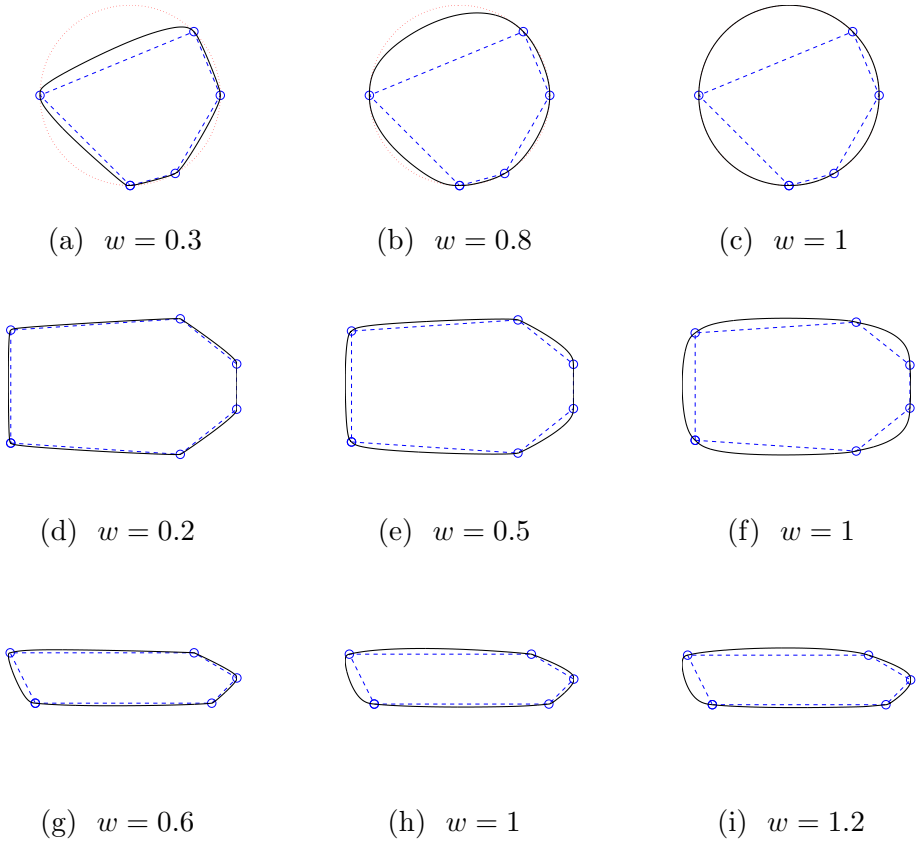

(a) $w = 0.3$ (b) $w = 0.8$ (c) $w = 1$

(d) $w = 0.2$ (e) $w = 0.5$ (f) $w = 1$

(g) $w = 0.6$ (h) $w = 1$ (i) $w = 1.2$

Fig. 9. The effect of changing the tension parameter when interpolating the same sequence of points and derivatives.

w the tightness of the limit curve is progressively increased, in correspondence of the value $w = 1$ the constructed subdivision scheme converges exactly towards the

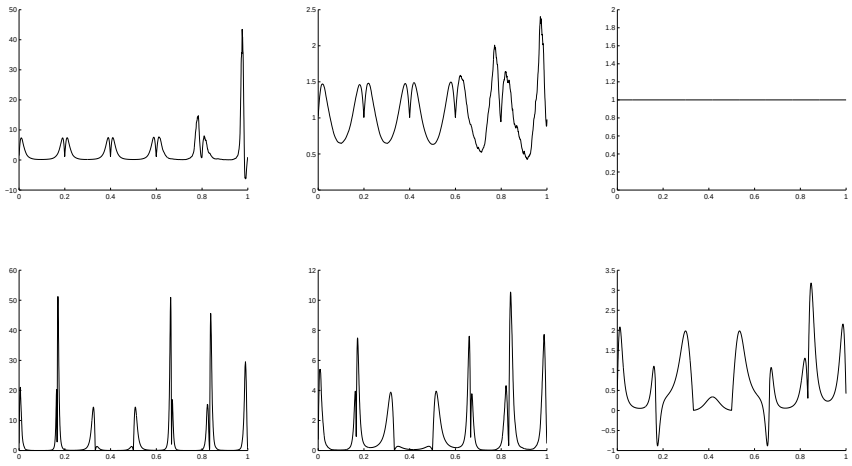

Fig. 10. Discrete curvature plots for the refined polylines in Fig. 9 (a)-(b)-(c) (first row) and in Fig. 9 (d)-(e)-(f) (second row) obtained after 10 steps of the proposed algorithm.

piecewise rational quintic Hermite interpolant. This model thus represents the first example of interpolatory curve subdivision that, for a certain value of the parameter, generates in the limit a piecewise interpolatory rational spline.
As concerns the smoothness order of the limit curves it produces, C^2 continuity is exclusively proved for the special value $w = 1$. Although curvature continuity can be conjectured for any other positive value of w (since empirically shown by a wide range of experiments), a detailed smoothness analysis of the proposed Hermite scheme has to be provided. This issue will be objective of our future researches since it requires the development of more general theoretical tools not available in the literature.

Acknowledgements

This research was supported by University of Milano-Bicocca, Italy.
The author thanks Serge Dubuc and Jean-Louis Merrien for their useful suggestions on the first version of this paper. Special thanks also go to Malcolm Sabin and the anonymous referees for their valuable comments.

References

[1] Beccari, C., Casciola, G., Romani, L., 2007. A non-stationary uniform tension controlled interpolating 4-point scheme reproducing conics, Computer Aided Geometric Design **24**(1), 1-9.

[2] Casciola, G., Romani, L., 2005. A piecewise rational quintic Hermite interpolant for use in CAGD. In: Dæhlen M., Mørken, K., Schumaker, L.L. (eds.), Mathematical Methods for Curves and Surfaces, Nashboro Press, Brentwood, TN., 39-49.

[3] Chalmovianský, P., Jüttler, B., 2007. A non-linear circle-preserving subdivision scheme. Advances in Computational Mathematics **27**, 375-400.

[4] Dyn, N., Levin, D., 1999. Analysis of Hermite-interpolatory subdivision schemes. In: Dubuc S. (ed.), Spline functions and the theory of wavelets, CRM Proc. Lecture Notes **18**, Amer. Math. Soc., 105-113.

[5] Dubuc, S., 2006. Scalar and Hermite subdivision schemes. Appl. Comput. Harmon. Anal. **21**, 376-394.

[6] Dubuc, S., Lemire, D., Merrien, J.-L., 2001. Fourier analysis of 2-point Hermite interpolatory subdivision schemes. The J. of Fourier Analysis and Applications **7**(5), 537-552.

[7] Farin, G., Nasri, A., 2001. A subdivision algorithm for generating rational curves. J. of Graphics Tools **6**(1), 35-47.

[8] Hohmeyer, M.E., Barsky, B.A., 1989. Rational continuity: parametric, geometric, and Frenet frame continuity of rational curves. ACM Transactions on Graphics **8**(4), 335-359.

[9] Merrien, J.-L., 1992. A family of Hermite interpolants by bisection algorithms. Numerical Algorithms **2**, 187-200.

[10] Merrien, J.-L., 1999. Interpolants d'Hermite C^2 obtenus par subdivision. M2AN Math. Model. Num. Anal. **33**, 55-65.

[11] Romani, L., 2009. From approximating subdivision schemes for exponential splines to high-performance interpolating algorithms. J. of Computational and Applied Mathematics **224**(1), 383-396.

[12] Sabin, M.A., Dodgson, N.A., 2005. A circle-preserving variant of the four-point subdivision scheme. In: Dæhlen M., Mørken, K., Schumaker, L.L. (eds.), Mathematical Methods for Curves and Surfaces, Nashboro Press, Brentwood, TN., 275-286.

[13] Yu, T. P.-Y., 2005. On the regularity analysis of interpolatory Hermite subdivision schemes. J. Math. Anal. Appl. **302**, 201-216.